



Synergistic action of electrolyzed water and mild heat for enhanced microbial inactivation of *Escherichia coli* O157:H7 revealed by metabolomics analysis

Qin Liu^{a,c}, Lin Chen^{a,c}, Anna Karen Carrasco Laserna^b, Yun He^{a,c}, Xiao Feng^{a,c}, Hongshun Yang^{a,c,*}

^a Department of Food Science & Technology, National University of Singapore, Singapore, 117542, Singapore

^b Department of Chemistry, National University of Singapore, Singapore, 117543, Singapore

^c National University of Singapore (Suzhou) Research Institute, Suzhou, Jiangsu, 215123, PR China

ARTICLE INFO

Keywords:

Escherichia coli
Electrolyzed water
Metabolomics
Omics
Pathway analysis
Bacterial response
Pathogen
Sanitization
Heat treatment
Non-thermal processing
UPLC-QTOF-MS/MS
Principal component analysis
Oxidative stress
PCR
Gene expression
Food microbial safety
Sanitizer
Chlorine
Inactivation

ABSTRACT

To determine the bactericidal mechanism of electrolyzed water and mild heat against *Escherichia coli* O157:H7, we performed ultra-performance liquid chromatography quadrupole time of flight mass spectrometry (UPLC-QTOF-MS/MS) coupled with multivariate analysis to profile the intracellular metabolites of *E. coli* O157:H7 in response to electrolyzed water (EW) and mild heat treatment. The results indicated that EW (4 mg/L free available chlorine) combined with heat treatment at 50 °C resulted in 2.31 log CFU/mL reduction of *E. coli* O157:H7 and the reactive oxygen species fluorescence intensity of EW at 50 °C was ten times higher than that of the control group. Data demonstrated that treatment with EW and heat caused significant perturbation of metabolic pathways that were functionally related with amino acid metabolism, nucleotides synthesis, and lipid biosynthesis. EW at 50 °C resulted in major alterations to pathways involved in acyl carrier protein metabolism, anhydromuropeptides recycling, biosynthesis of CDP-diacylglycerol, trehalose and lipid IVa. Transcriptome analysis revealed that heat and EW affected the transcription levels of some genes in opposite ways. The expression of *rpoS*, *oxyR*, *soxR*, *gadA*, *gadB*, *sucA*, and *sucB* in the 50 °C group was downregulated, but upregulated in EW exposed cells. The expression of most genes was reduced in response to the combined treatment, with 0.024- and 0.286-fold downregulation of *udk* (encoding uridine kinase) and *gadA* (encoding glutamate decarboxylase alpha), respectively, being observed in cells treated with EW at 50 °C. These results provided further evidence of the metabolomic and transcriptomic response of *E. coli* O157:H7 to oxidation and heat stress.

1. Introduction

Bacterial infections, because of their potential as health hazards, have become a cause for public health concern (Endersen et al., 2015). The use of disinfection in the food and agricultural industries is a common practice to reduce the microbial population and increase the shelf life of food products. *Escherichia coli* O157:H7 is a pathogen that commonly causes foodborne illness, often from the consumption of contaminated fruit and vegetables (Adhikari, 2018; Cui, Bai, Yuan, Surendhiran, & Lin, 2018; Han et al., 2018; Ngnitcho et al., 2018). Various sanitization techniques have been adopted by the food industry to improve the microbial safety and quality of fresh produce (Fisher et al., 2016; Joshi, Salvi, Schaffner, & Karwe, 2018; Montville &

Schaffner, 2004).

Recent studies have highlighted that electrolyzed water (EW) is one potential substitute for traditional chlorine washing (Gil, Gómez-López, Hung, & Allende, 2015; Liu, Jin, Feng, Yang, & Fu, 2019; Liu, Tan, Yang, & Wang, 2017; Tango, Mansur, Kim, & Oh, 2014). EW has a high oxidative reduction potential (ORP) and acts as oxidative agent to disrupt cellular functions, including DNA synthesis, permeable membrane structure, metabolic enzymes, and electron transport systems. In addition, chlorine on the produce surfaces may contribute to a higher bacterial reduction due to the unfavorable condition for the colonization and survival of the bacteria (Chhetr, Janes, King, Doerrler, & Adhikari, 2019). However, the ORP in wash water and the disinfecting efficacy may be decreased because of the presence of soil and other

* Corresponding author. Department of Food Science & Technology, National University of Singapore, Singapore, 117542, Singapore.

E-mail address: fstynghs@nus.edu.sg (H. Yang).

<https://doi.org/10.1016/j.foodcont.2019.107026>

Received 17 September 2019; Received in revised form 26 November 2019; Accepted 27 November 2019

Available online 29 November 2019

0956-7135/ © 2019 Elsevier Ltd. All rights reserved.

organic load matters on produce surfaces. As a consequence, *E. coli* O157:H7 cells may survive and adapt to sublethal oxidative stress by initiating defense mechanisms against subsequent stress conditions during infection in the human gastrointestinal tract (Zook, Busta, & Brady, 2001). Measuring metabolite levels and the variation in bacteria can provide insights into the response of bacteria to disinfection intervention. Metabolomic investigation has been shown to be a promising method to identify metabolic changes of bacteria in response to oxidative stress, and could provide new insights into the biological process of the stress response (Chen, Zhao, Wu, He, & Yang, 2020; ; Liu et al., 2017, b; Zhao, Zhao, Wu, Lou, & Yang, 2019).

Recently mass spectrometry (MS) has become popular in metabolic profiling, as improvements to both instrumentation and software make it more feasible to acquire high-throughput profiles of bacteria metabolic status to enhance our knowledge of the mechanisms underlying oxidative stress and the resulting bacterial response (Fei, Bowdish, & McCarry, 2014; Zampieri, Sekar, Zamboni, & Sauer, 2017). Liquid chromatography (LC) separation before MS can reduce the complexity of the mass spectra and provide useful information on metabolites' physicochemical properties, which may help in their identification (Holmes et al., 2010). MS has emerged as a revolutionary technique for the rapid identification of microorganisms and could be widely used for bacterial and fungal pathogens identification in clinical microbiology laboratories. Work by Tam et al. (2014) found that metabolic fingerprinting of *Aspergillus flavus*, *A. nomius*, and *A. tamarii* strains could separate three hierarchical clusters based on ultra-high-performance liquid chromatography-tandem mass spectrometry (UHPLC MS).

Although many studies have proven the effectiveness of EW as an antimicrobial agent, there are little data on the metabolic response and adaptation of *E. coli* O157:H7 to sublethal concentrations of EW disinfection treatment. To gain comprehensive insights into the metabolic responses, we analyzed the metabolite composition in conjunction with gene expression of *E. coli* O157:H7 in response to EW and heat treatment.

2. Materials and methods

2.1. Bacterial strains and culture conditions

E. coli O157:H7 EDL 933 (derived from ATCC strain 43895), *Escherichia coli* O157:H7 ATCC 35150 and *E. coli* ATCC 25922 were obtained from Department of Food Science & Technology, National University of Singapore. Frozen stock cultures were activated in 10 mL of sterile tryptic soy broth (TSB, Oxoid, Basingstoke, UK) for 18–24 h at 37 °C. After two consecutive transfers for 18–24 h at 37 °C, working cultures at stationary phase were used for the experiments.

2.2. Oxidative stress treatment

An overnight culture (2 mL) was washed twice and resuspended in phosphate-buffered saline (PBS). A 1-mL aliquot each of *E. coli* O157:H7 EDL 933 and non-O157 *E. coli* ATCC 25922 cultures was inoculated into 100 mL of pre-warmed TSB with subsequent incubation at 37 °C for 3.5 h to reach exponential phase (OD₆₀₀ = 0.5). Subsequently, 9.5 mL of culture was added to the treatment test tube containing 0.5 mL EW (4 mg/L final free available chlorine). Controls contained an equivalent volume of distilled water. Both treatment and control samples were incubated for 5 min at 37 °C or 50 °C.

2.3. Survival analysis

For bacterial viability studies, *E. coli* O157:H7 EDL 933, *E. coli* O157:H7 ATCC 35150 and *E. coli* ATCC 25922 cells were cultivated in TSB media until an OD₆₀₀ of 0.5. Bacteria cells was harvested by centrifugation at 5000 × g for 10 min and washed with PBS (pH 7.5). The bacterial culture was added to a test tube under different conditions

(three temperatures: 40, 50, and 60 °C). Temperatures were adjusted using incubators and a water bath. Following each treatment, 1 mL of each sample was transferred to a tube containing 9 mL of neutralizer (0.85% NaCl containing 0.5% Na₂S₂O₃). Serial ten-fold dilutions were performed in 0.1% peptone and surviving populations were evaluated by enumeration on triplicate tryptic soy agar (TSA, Oxoid, Basingstoke, UK) plates at 37 °C for 24 h.

2.4. Detection of intracellular reactive oxidative species (ROS)

The oxidant-sensitive probe 2', 7-dichlorodihydrofluorescein diacetate (H₂DCFDA) was used to assess the intracellular ROS levels. Briefly, 1 mL of *E. coli* O157:H7 EDL 933 or *E. coli* 25922 at approximately 10⁸ cells/mL were pre-incubated with 200 μM H₂DCFDA in the dark at 37 °C for 30 min. The bacteria were then washed, and re-suspended in 1 mL of PBS buffer. The bacterial suspension was then treated with EW (free available chlorine 0.4 mg/L) at different temperatures for 5 min. Sodium thiosulfate (Sigma-Aldrich, Co., St. Louis, MO, USA) at a final concentration of 0.5% w/v was added to neutralize the excess EW after 5 min of treatment. Cells were washed, centrifuged at 6000 × g for 10 min, resuspended in buffer, and disrupted by sonication. For all control and treated groups, 100 μL of the bacterial suspension were transferred into each well of a 96-well plate (Corning, Tewksbury, MA, USA). The fluorescence intensity was measured at excitation/emission wavelengths of 488/520 nm using a fluorescence plate reader (Spectrafluor Plus, Tecan, Durham, NC, USA) (Liu et al., 2018). All conditions were tested in triplicate.

2.5. Extraction of intracellular metabolites

The extraction of intracellular metabolites was performed according to a method described by (Lu, Kimball, & Rabinowitz, 2006) with minor modifications. Briefly, *E. coli* O157:H7 EDL 933 or *E. coli* 25922 cells (9.5 mL) were either control (0.5 mL DW) or stressed (0.5 mL of EW or NaClO, final free available chlorine (FAC) level of 4 mg/L) with short vortex duration. After 5 min of treatment at 25 or 50 °C, the cell cultures were quenched by a brief incubation on ice and washed with 0.9% (w/v) NaCl solution three times. Cell pellets were suspended in 300 μL of 80:20 methanol:water at dry ice temperature (−75 °C). After 15 min at −75 °C, the mixture was centrifuged in microfuge for 5 min at 6000 × g at 4 °C. Cell pellets were then resuspended in 300 μL of extraction solution and sonicated (80 kHz, 100 w) for 25 cycles, with each cycle consisting of 5 s pulse and 10 s stops. The resulting pellet was re-extracted twice with 200 μL of solvent at 4 °C. All three of the supernatant were combined to yield 700 μL of final extract. The samples were stored at −80 °C for further analysis. Five replicate samples were taken for each treatment.

2.6. UPLC/Q-TOF-MS measurement

The metabolites were quantified using an Agilent 1290 Infinity LC System (Agilent, Germany), using an Acquity HSS T3 column (1.8 μm, 2.1 × 30 mm; Waters, Manchester, UK). The column oven temperature was maintained at 40 °C, and the auto-sampler temperature was maintained at 4 °C. The mobile phase was (A): 0.1% formic acid in water and (B) 0.1% formic acid in acetonitrile. The linear gradient program began with 1% B for 0.5 min; 0.5–1.5 min increase in B from 1% to 20%; 1.5–3 min increase in B from 20% to 50%; 3–4.5 min increase in B from 50% to 95%; 4.5–5 min held at 95% B; and 5–7.5 min (postacquisition time) starting mobile phase 1% B to re-equilibrate the column. The flow rate was 400 μL/mL and the injection volume was 1.5 μL. Mass spectrometry was performed using an Agilent 6540 Accurate-Mass Q-TOF (Agilent, Germany). Ionization was performed in both positive and negative electrospray (ESI) mode. The mass range was set at *m/z* 50–1000 Da with a 0.3 s scan time. The ESI source conditions were as follows: capillary voltage, 4.0 kV (ESI+) and 2.4 kV

(ESI⁻); source temperature, 120 °C; and desolvation temperature, 350 °C. Nitrogen was used as the desolvation and cone gas with a flow rate of 180 L/h (Holmes et al., 2010).

Data analysis was performed in XCMS according to previously described methods (Farrés, Piña, & Tauler, 2016). All the UPLC-MS raw files were converted to mzML format, and the converted files were imported to the XCMS software for non-linear alignment in the automatic integration, time domain, and extraction of the peak intensities. Principal component analysis (PCA) was used as the classification method for modeling the discrimination between the control and treatment groups based on intracellular metabolites. The peaks in the control samples were compared with those in the EW or heat treatment samples. Potential metabolites biomarkers were extracted using statistically significant threshold of fold values larger than 1.5 (up- or downregulation). The metabolites with fold values larger than 1.5 and *p* value less than 0.05 were selected. Metabolites were assigned and identified by using Metlin based on their MS signature and tandem mass spectrometry (MS/MS) spectra. Metabolite pathway analysis was performed using XCMS and MetaboAnalyst tools.

2.7. RNA isolation and quantitative real-time reverse transcription-PCR (qRT-PCR) analysis

Culture aliquots were collected and quickly stabilized by adding two volumes of RNeasy Protect Bacteria Reagent (Qiagen, Hilden, Germany) and incubating at room temperature for 5 min. Total RNA was extracted from cells using an RNeasy Mini Kit (Sangon Biotech, Shanghai, China) according to the manufacturer's instructions. The RNA concentration and purity were assessed spectrophotometrically using a Nanodrop 1000 instrument (Thermo Scientific Inc., Wilmington, DE, USA), and its integrity was checked by agarose gel electrophoresis. One microgram of RNA was reverse transcribed into cDNA using a Reverse Transcription Kit (Sangon Biotech, Shanghai, China). Relative expression was assayed in a reaction mixture containing 10 µL of Luna Universal qPCR Master Mix, 1 µL of forward primer, 1 µL of reverse primer, 1 µL of template cDNA, and 7 µL of PCR water. Quantitative real-time PCR (qPCR) was performed using StepOnePlus Real-Time PCR System (Applied Biosystems, Carlsbad, CA, USA) to evaluate the transcription levels of stress-related genes. Thermal cycling conditions comprised of 1 cycle at 95 °C for 20 s; followed by 40 cycles at 95 °C for 3 s and 60 °C for 30 s. The expression of 16s rRNA was used as the endogenous control. Detailed information concerning the target genes and primer sequences is presented in Table 3. The relative changes in gene expression were calculated using the $2^{-\Delta\Delta C_t}$ method (Livak & Schmittgen, 2001).

2.8. Statistical analysis

Mean values for all parameters were calculated from the independent triplicate trials. The results were analyzed using one-way analysis of variance (ANOVA) in the statistical software SPSS v18 (Statistical Package for the Social Sciences, Chicago, IL, USA). Differences between means were subject to Duncan's test and a difference with *P* < 0.05 was considered significant.

3. Results and discussion

3.1. Survival of *E. coli* O157:H7 and *E. coli* after EW and heat treatments

The cells of non-pathogenic *E. coli* and pathogenic *E. coli* O157:H7 were subject to the EW and mild heat treatment. The survival of populations of non-pathogenic *E. coli* and pathogenic *E. coli* O157:H7 EDL 933 under different treatment conditions are shown in Fig. 1. The survival results for *E. coli* O157:H7 treated at 40 and 50 °C showed no significance difference compared with that of the control group. Treatment at 60 °C resulted in a significantly greater (*P* < 0.05) sanitizing effect (3.78 log CFU/mL reduction) than treatment at 40 °C

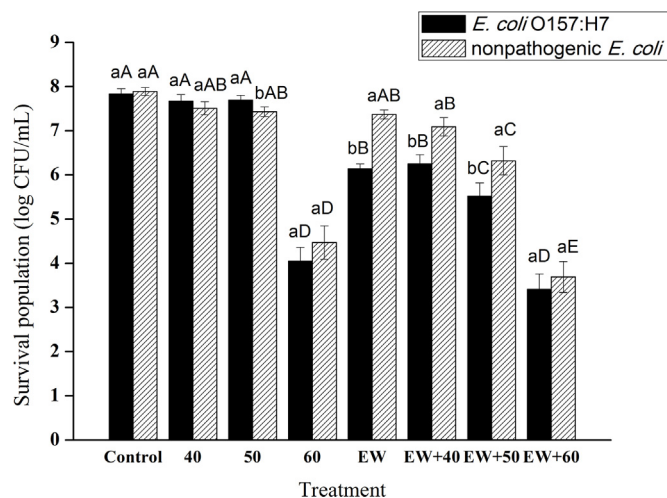


Fig. 1. Survival of *Escherichia coli* O157:H7 EDL 933 (A) and nonpathogenic *E. coli* (B) treated with electrolyzed water (EW) and mild heat (*n* = 3). Means with different lowercase letters (a, b) represent significant differences among *E. coli* O157:H7 EDL 933 and nonpathogenic *E. coli* in a particular treatment, whereas means with different capital letters (A, B, C) represent significant differences among the treatments with regard to a particular strain at *P* ≤ 0.05, according to Duncan's test.

(0.16 log CFU/mL reduction) and 50 °C (0.14 log CFU/mL reduction) compared with the untreated control. The same trend occurred with the addition of EW; the sanitizing effect of EW combined with heat treatment at 60 °C (4.14 log CFU/mL reduction) was greater than that at 50 °C (2.31 log CFU/mL reduction) (Fig. 1A). The survival results of *E. coli* O157:H7 ATCC 35150 showed similar trend indicating the synergistic effect from the cooperation of EW and mild heat (Fig. S1). However, since only pure culture was used in this study, future work on of sanitization potency on produce should be conducted considering the organic matter (Chen & Hung, 2017) and different cell attachment levels on produce surfaces (Chhetri et al., 2019).

At the same time, the sanitizing effect of EW at all temperatures was significantly greater than the sanitizing effect of heat treatment alone. For example, treating *E. coli* O157:H7 EDL 933 cells with EW at 50 °C resulted in a significantly greater sanitizing effect (2.31 log CFU/mL reduction) than treatment at 50 °C without the addition of EW (0.14 log CFU/mL reduction). However, at 60 °C, whether or not EW was added had no statistically significant impact on the sanitizing effect. For *E. coli* O157:H7 treated at 60 °C, the sanitizing effect was a 3.78 log CFU/mL reduction, which was similar to those treated with EW combined with 60 °C (4.14 log CFU/mL reduction).

The effects of different temperatures (40, 50, 60 °C) and EW treatments on non-pathogenic *E. coli* survival are shown in Fig. 1B. A similar trend was observed in non-pathogenic *E. coli* to those of *E. coli* O157:H7 EDL 933. The combination of EW with 50 °C was chosen for the following investigations because it showed a synergistic effect: The sanitizing effect was higher than the sum of the individual effects.

3.2. Measurement of intracellular reactive oxidative species (ROS)

To investigate the ROS production upon heat and EW treatments, cells were incubated with a generic probe H₂DCFDA, and the interaction of H₂DCFDA with ROS was presented as the fluorescence intensity. The cells of both *E. coli* O157:H7 EDL 933 and nonpathogenic *E. coli* were treated at different temperatures. At 50 °C, cells with or without EW treatment were analyzed.

The fluorescence intensity of the H₂DCFDA-labeled cells increased with respect to the control cells, which indicated the heat activation of fluorescent dye molecules by peroxide molecules and hydroxyl radicals (Fig. 2). The fluorescence intensity of EW at 50 °C was the highest, at 10

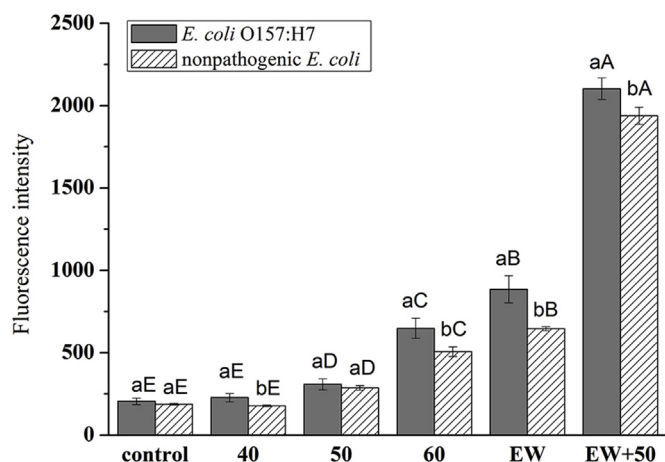


Fig. 2. Effect of electrolyzed water (EW) and mild heat on intracellular ROS accumulation in *Escherichia coli* O157:H7 EDL 933 and nonpathogenic *E. coli*. Means with different lowercase letters (a, b) represent significant differences among *E. coli* O157:H7 EDL 933 and nonpathogenic *E. coli* in a particular treatment, whereas means with different capital letters (A, B, C) represent significant differences among the treatments with regard to a particular strain at $P \leq 0.05$, according to Duncan's test.

times the value of the control group. Our results suggested that the formation of ROS upon EW treatment was significantly enhanced by heating, as a consequence of destabilization of the cellular structure or loss of activity of cellular defense systems (Marcén, Ruiz, Serrano, Condón, & Mañas, 2017).

3.3. Metabolomic profiling and pathway analysis

To explore the possible mechanism underlying the changes in bacterial oxidative and heat responses, metabolite profiles were investigated. The present study was designed to compare and identify patterns of biochemical changes between control and stressed *E. coli* O157:H7 EDL 933, and to determine if a LC-MS-based metabolomics approach could be used successfully as a high-throughput tool for pathogen research. To the best of our knowledge, this is the first study to evaluate metabolite profiles and pathways to investigate the oxidative response of *E. coli* O157:H7 EDL 933 cells using UPLC-QTOF-MS.

Samples were analyzed using a UPLC-MS platform, which is appropriate for the detection of a wide range of low-molecular-weight metabolites. Metabolites containing only C, H and O may be considered to be detected by the negative ion mode in LC-MS, whereas metabolites that also contain N, would be expected to be preferentially ionized in the positive-ion mode. Therefore, ionization should be carried out in both positive and negative modes to enhance metabolome coverage.

Metabolite profiling from *E. coli* O157:H7 was performed by UPLC-MS/MS in conjunction with XCMS data analysis methods. For multivariate analysis, principal component analysis (PCA) showed that 36% and 31% of total variance in the data were represented by the first two principal components, which were negative ion mode and positive ion mode, respectively. The 2D-PCA score (Fig. 3) plots revealed that all the intracellular metabolites of treated *E. coli* O157:H7 EDL 933 could be distinguished from the untreated control group on the first two principal components, and the EW and heat treated cells were clearly separated from the control cells along PC1, which represented 24% and 17% of variance for negative and positive ion mode, respectively.

The extracted samples were analyzed by reverse-phase liquid chromatography coupled to electrospray ionization (ESI) in both positive mode (+) and negative mode (-). The identification of metabolites could be a significant challenge in MS-based profiling. The use of MS/MS provides useful information on fragmentation for identification purpose. Quadrupole time-of-flight (QTOF) mass spectrometry can

provide high mass-accuracy measurements of precursor ions and their product daughter ions. The analysis of *E. coli* O157:H7 EDL 933 metabolic extracts revealed the presence of identical or highly similar compounds, indicating a conserved class of biochemical compounds among the different treatments (Fig. S2).

Together, LC-MS with XCMS allowed us to detect changed metabolic features in *E. coli* O157:H7 EDL 933 and nonpathogenic *E. coli* cells. Among the lists of metabolites altered by heat and EW, the levels of 78 and 112 metabolites from positive and negative modes, respectively, were significantly changed after the combined treatment. By comparing the metabolic features between combined treatment and EW or heat individually, the synergistic effects of the most significant changes could be identified. Our analysis indicated that the alteration in the metabolic features were distinct between the *E. coli* O157:H7 and nonpathogenic *E. coli*.

An untargeted metabolomics approach was applied to determine the metabolites in extracts of control and treated cells. Paired analysis revealed the alteration of metabolites. Metabolic analysis of EW and heat-treated cells indicated that several metabolites were differentially regulated in *E. coli* O157:H7 EDL 933 (Table 1). The analysis showed that EW and heat have different effects at the biochemical level. Meanwhile, the combination of EW and heat treatment resulted in the most marked alterations. The statistically important variables (ions) related to EW and heat treatment were screened via spectrum deconvolution and alignment of mass ions from data files into a single data set using XCMS. The ions with altered intensities are represented in cloud plots (Fig. 4).

The dysregulated features of heat, EW treatment, and combined treatment are shown in the mirror plot (Fig. 4). The ion intensities are shown in circles with statistical thresholds set at p -value < 0.01 and fold change > 2 . Features that are upregulated are shown as circles on the top of the plot, whereas features that are downregulated are shown as circles on the bottom. Variables with a p -value less than 0.01 and a fold value larger than 1.5 were considered as potential markers representing the metabolic characteristics of EW and heat treatments. Significant synergies were observed in the combined treatment group (Fig. 4c). When comparing the intracellular metabolites from treated samples with the controls, variations in several metabolites (i.e., arginine, L-asparagine, phenylalanine, phosphatidylglycerol, UDP-glucose, citric acid, uridine, guanosine, and cytidine triphosphate) were observed (Tables 1 and 2).

To expand our understanding of the biological meaning of the results, the interconnectivity of metabolites in biological pathways can be inferred using network enrichment analysis. A p -value ≤ 0.05 is considered to indicate strong enrichment in the annotation categories. Significant pathways in the cells treated with EW combined with heat were revealed by setting the statistical threshold at $p < 0.05$ (Fig. 5). The pathways were functionally related with amino acid metabolism, nucleotides synthesis, and lipid biosynthesis. The metabolites were integrated and summarized to produce a simplified schematic metabolic map using literature data and the Kyoto encyclopedia of genes and genomes (KEGG) database (Fig. 6). Our analysis showed that EW and mild heat have distinctively different effects on metabolic flux (Fig. 6). The key metabolic pathway altered by EW exposure involved amino acid synthesis and nucleic acid synthesis. *E. coli* can use four naturally occurring purine ribonucleosides (xanthosine, adenosine, guanosine, and inosine) as sources of carbon and energy, yielding D-ribose-5-phosphate, which, can be converted for the synthesis of nucleotides and nucleic acids (Horinouchi et al., 2006). Ribose-5-phosphate is an intermediate of the pentose phosphate pathway and is a precursor for the synthesis of nucleotides (Stincone et al., 2015). The changes in the ribose-5-phosphate level strongly indicated an effect on nucleotide biosynthesis, which was consistent with nucleotide levels (e.g., uridine, guanosine) in the *E. coli* O157:H7 cells in response to EW and heat treatments. Lipopolysaccharide is one of the major components of cell membranes and lipid IVA is the precursor of lipid A, the core lipid-

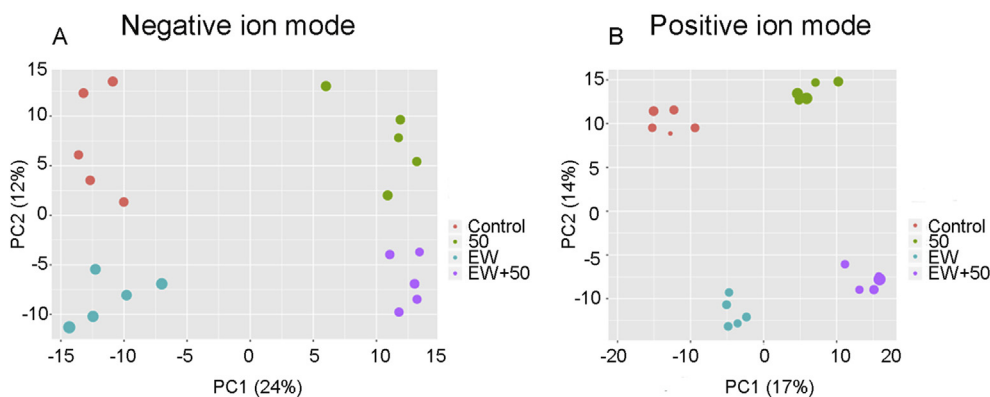


Fig. 3. Principal component analysis (PCA) plots for metabolomics data generated using UPLC-MS in negative and positive ion modes. (A) Negative ion mode; (B) Positive ion mode. EW, electrolyzed water; 50, 50 °C.

Table 1

List of metabolites in control and treated *E. coli* O157:H7 cells.

Class	Metabolites	Fold Change		
		50	EW	EW+50
Amino acid metabolism	Arginine	-2.0	-1.2	-3.4
	Asparagine	1.0	1.3	1.8
	Phenylalanine	-1.4	-1.5	-1.5
Glycerophospholipids	PG(13:0/22:1(11Z))	1.4	1.2	5.0
	PA(O-18:0/18:3(6Z,9Z,12Z))	1.2	2.6	5.0
	PA(P-20:0/17:2(9Z,12Z))	8.5	3.2	5.2
	UDP-glucose	10.1	-1.3	10.5
Carbohydrate related	Citric acid	3.5	3.2	3.2
	Uridine	10.1	1.1	10.5
Nucleosides and nucleotides	Guanosine	5.4	41.5	44.3
	Cytidine triphosphate (CTP)	10.8	4.9	31.9

PG, phosphatidylglycerol; PA, phosphatidic acid; UDP, uridine diphosphate.

Table 2

List of metabolites in control and treated nonpathogenic *E. coli* cells.

Class	Metabolites	Fold Change		
		50	EW	EW+50
Amino acid metabolism	Arginine	-1.1	-1.2	-1.8
	Asparagine	-3.2	-1.4	-2.7
	Alanine	-2.1	-1.2	-2.3
Glycerophospholipids	PG(16:0/16:1(9Z))	-4.7	1.2	-6.1
	PG(22:0/22:2(13Z,16Z))	1.2	-1.2	-1.4
	MG(18:2(9Z,12Z)/0:0/0:0)	1.3	1.2	3.1
Carbohydrate related	UDP-glucose	10.1	-1.3	10.5
	Citric acid	3.5	3.2	3.2
	Succinate	-1.8	1.5	3.6
	gamma-Aminobutyric acid	-1.1	1.7	1.6
Nucleosides and nucleotides	Uridine	-1.3	-1.1	-2.1
	Guanosine	1.1	-1.5	-4.2
	Cytidine triphosphate (CTP)	4.8	5.5	11.6

PG, phosphatidylglycerol; MG, monoacylglyceride; UDP, uridine diphosphate.

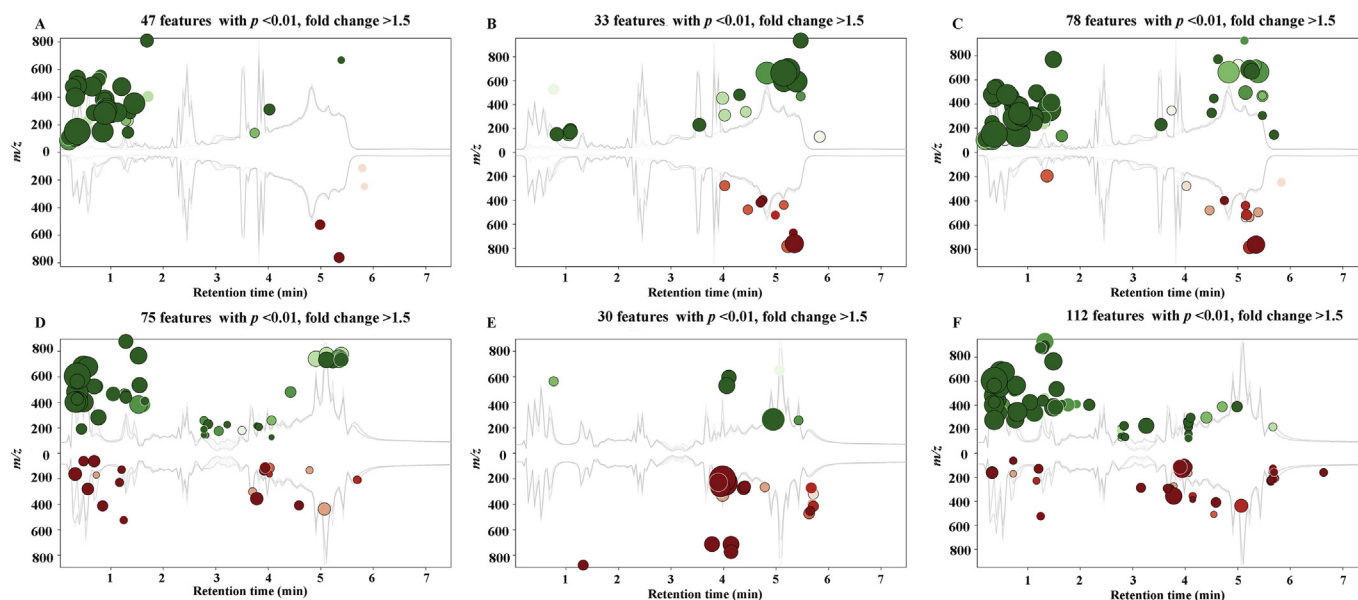


Fig. 4. Cloud plots present the metabolite features of *Escherichia coli* O157:H7 EDL 933. Depicted are [+] and [-] ions whose intensities between groups were altered > 1.5-fold with a P value < 0.01. Ions that were upregulated are represented as green circles above the plot, and those that were downregulated are represented as red circles below the plot. The size of each circle corresponds to the log-fold change of the ion, and the shade of the circle represents the p value, with brighter circles having a lower p value. (For interpretation of the references to colour in this figure legend, the reader is referred to the Web version of this article.)

Table 3
Primers used in real-time PCR reactions in this study.

Gene	Gene/protein annotation	Sequence (5'-3')
<i>oxyR</i>	hydrogen peroxide-inducible genes	F: GAAGCACAGACCCACAGTT R: CAAACAAACGGCACTTCAATG
<i>soxR</i>	Redox-sensing activator of <i>soxS</i>	F: CGTAACAGCGGCAATCAGC R: ACGCCAAACGCTTACCAAT
<i>rpoH</i>	RNA polymerase sigma factor RpoH	F: CCACAGGCGGATTTGATTC R: GGTTTGCCGCCTGCTTCT
<i>rpoS</i>	RNA polymerase sigma factor RpoS	F: AATCGTGGTCTGGCGTTGC R: GCGTATGTTGAGAAGCGGAAAC
<i>osmB</i>	Osmotically inducible lipoprotein	F: AAATGACCGCGGCTGTTC R: TTATTTACCGACCTGGTGACCAAT
<i>gadA</i>	Glutamate decarboxylase alpha	F: GGACCAGAAGCTGTTAACGGATTT R: GCGATAGTAGAAATGGCCTTTGC
<i>gadB</i>	Glutamate decarboxylase beta	F: GATTCAGGTTTTGGTGCGAAGT R: ACGAGCGTTGCCATCAAGATATAAT
<i>icdA</i>	Isocitrate dehydrogenase	F: GACCGAAGCGGCTGACTTAA R: GCAGTTTAGCGCCATCCATC
<i>sucA</i>	2-oxoglutarate dehydrogenase E1 component	F: GCGGCAAAGAAACCATGAAA R: TCGGTGCTGGTAATGTGCA
<i>sucB</i>	SucB- dihydrolipeate	F: GCAGTACGGTGAAGCGTTTG R: CTTCCGGGTAACGTTTCAGG
<i>udk</i>	Uridine kinase	F: TTTGGATCCATGACTGATCAGTCTCACCAGTG R: ATCAAGCTTATTCAAAGAAGTACTTATTTCGTT
16s rRNA		F: AGAGGATGACCCAGCCACAC R: CGGGTAACGTCAATGAGCAAAG

^a Primers are described in Wang et al. (2009) and Sheridan, Masters, Shallcross, and Mackey (1998).

linked oligosaccharide consisting of an inner and outer region. The presence of hypochlorous acid and hydrogen peroxide, which in turn results in hydroxyl radical formation, could arise from oxidizing ROS in biological systems (Bolin & Cardozo-Pelaez, 2007; Stan, Woods, & Daeschel, 2005). The interaction of ROS with cellular DNA has the potential to induce harmful effects and a number of possible DNA lesions. Oxidation of guanosine has been considered a hallmark biomarker to assess oxidative stress because it has the lowest oxidation potential among the four DNA bases and is the most readily oxidized, mostly in the formation of 8-hydroxy-2'-deoxyguanosine, which is the product of two-electron oxidation (Bolin & Cardozo-Pelaez, 2007; Milligan, Aguilera, & Ward, 2001). EW induced the conversion of uridine-based nucleotides to cytidine-based nucleotides, which involves the phosphorylation of the de novo-synthesized UMP to UTP and its conversion to CTP. Methionine is prone to be oxidized in proteins and may be attacked by ROS generated in biological systems (Stadtman, Moskovitz, Berlett, & Levine, 2002). It was not surprising that the methionine degradation pathway was affected after EW incubation, thus it may function in intermediate protection against ROS. As previously described, interconversion of antioxidants plays an important role in the cellular reduction system and in bacterial defense against oxidative stress (Ezraty, Gennaris, Barras, & Collet, 2017; Levine, Moskovitz, & Stadtman, 2000). Recent research on the heat stress response of bacteria has been based on transcriptomic and metabolomics analysis, which showed that various amino acids were significantly accumulated or reduced after heat stress. The histidine kinase pathway was found contribute to the general stress response of bacteria under heat shock (Kaczmarczyk, Hochstrasser, Vorholt, & Francez-Charlot, 2015).

A synergistic effect *E. coli* O157:H7 EDL 933 after combined treatment majorly resulted in the pathway alteration involved CDP-diacylglycerol biosynthesis, acyl carrier protein metabolism, trehalose biosynthesis, anhydromuropeptides recycling, and lipid IVA biosynthesis. The osmotic strength of the cytoplasm in *E. coli* is regulated by organic molecules like glycine betaine, whose synthesis relies on external supply of betaine, choline, or proline. As shown by (Sévin & Sauer, 2014), when these extracellular compatible solutes are not available, bacteria cells can modulate their osmotic pressure via the accumulation of trehalose. Thus, the alteration of trehalose biosynthesis

indicated disruption of the osmotic strength after EW treatment at 50 °C. Lipid IVA is the precursor of lipid A, which is a core membrane component consisting of an inner and outer region. Our analysis showed alteration of Lipid IVA biosynthesis, indicating the growth and permeability defects upon combined treatment (Mansilla & de Mendoza, 2017). These results are of particular interest considering that oxidative stress combined with heat has disrupts the integrity of the membrane of *E. coli* O157:H7 cells.

3.4. Changes in stress-related gene expression

We next investigated the transcription levels of *oxyR*, *soxR*, *rpoH*, *rpoS*, *osmB*, *gadA*, *gadB*, *icdA*, *sucA*, *sucB*, and *udk* in *E. coli* O157:H7 EDL 933 and nonpathogenic *E. coli* treated with EW, heat, and the combined treatment to determine if these genes contributed to the different responses. The genes investigated in this study were chosen based on our previous work (Liu et al., 2018) and related papers (Mei, Tang, Carey, Bach, & Kostrzynska, 2015; Wang et al., 2009). The results indicated that except *rpoH*, almost all the genes the expression levels of all these genes were reduced in response to the combined treatment (Fig. 7). The induction of *rpoH*, encoding the heat shock promoter-specific σ_{32} subunit of RNA polymerase, would positively direct the transcription of genes encoding molecular proteases and chaperones involved in the folding of heat damaged polypeptides or their degradation in the cytoplasm, which is a protective mechanism that may render bacteria cells more resistance to subsequent heat treatment (Chung, Bang, & Drake, 2006; Yang, Khoo, Zheng, Chung, & Yuk, 2014).

The results demonstrated that heat treatment and EW affected the transcription levels of these genes in opposite ways. The expression levels of *rpoS*, *oxyR*, *soxR*, *gadA*, *gadB*, *sucA* and *sucB* in the 50 °C group were downregulated, while they were upregulated in EW exposed cells. EW induced high ROS levels, which lead to elevated levels of *rpoS*, *oxyR*, *soxR*, *osmB*, *gadA*, *gadB*, *sucA*, and *sucB*. A 50-fold increase in heat shock regulatory gene *rpoH* was found in the 50 °C and combination groups, while its expression in the EW group remained unchanged. Approximately 0.024- and 0.286-fold downregulation of *udk* (encoding uridine kinase) and *gadA* (encoding glutamate decarboxylase alpha) were observed in *E. coli* O157:H7 EDL 933 cells treated with EW at 50 °C.

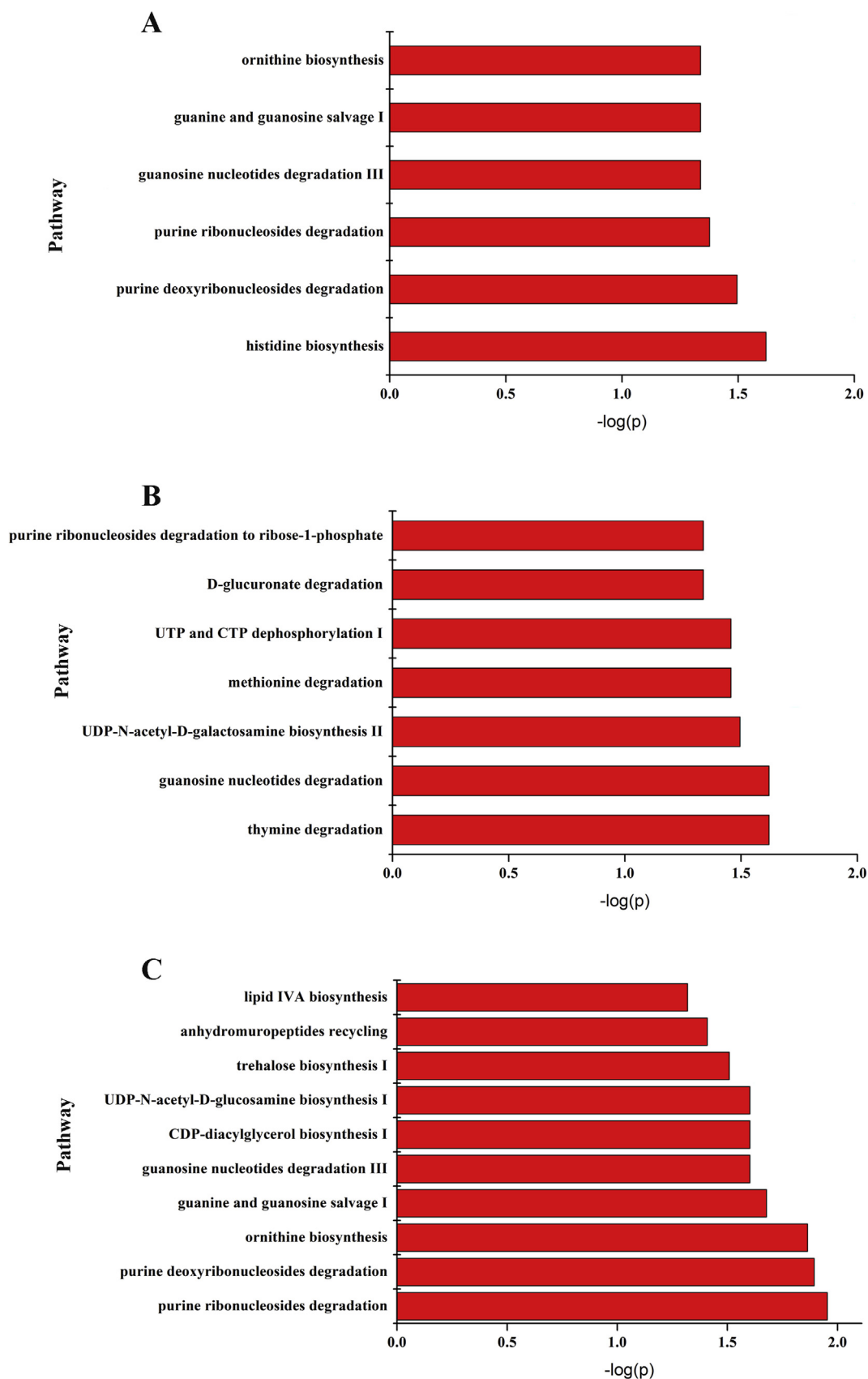


Fig. 5. Summary plot of the metabolite enrichment analysis of *Escherichia coli* O157:H7 EDL 933 upon heat (A), electrolyzed water (EW) (B), and combined (C) treatment.

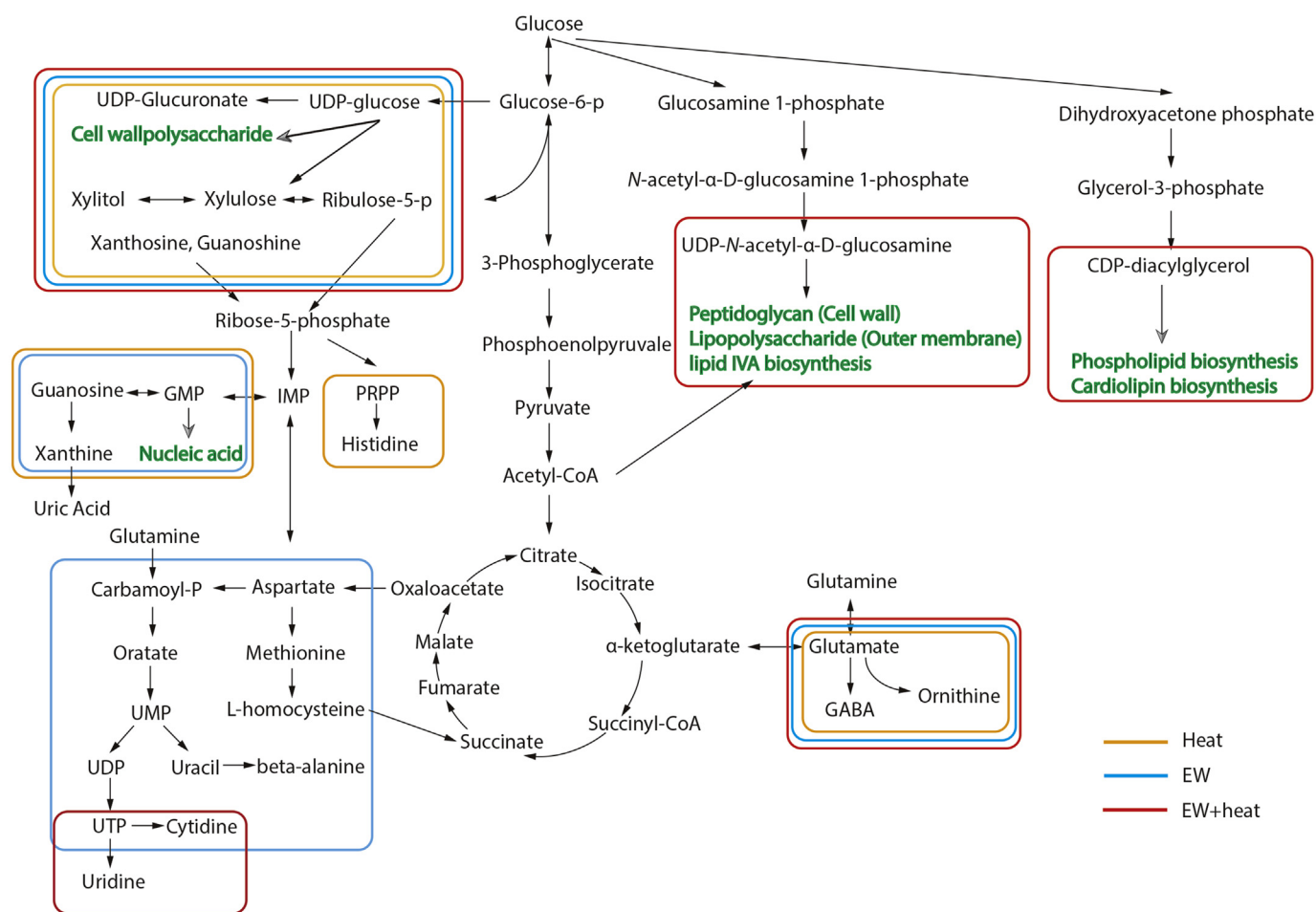


Fig. 6. Overview of pathways perturbed by electrolyzed water (EW) and heat in *Escherichia coli* O157:H7 EDL 933. Major pathways significantly affected upon EW, heat, and combined treatment are boxed in blue, yellow, and red respectively.

A variety of cellular responses to oxidative stress have been described, such as the expression of gene constituting the *oxyR*, *soxR*, and *rpoS* regulons (Mei et al., 2015). The products of the *soxR* and *oxyR* regulated genes, such as superoxide dismutase and catalases, are involved in defense against oxidative damage by modulating the levels superoxide-generating compounds and hydrogen peroxide, respectively. Uridine kinase is involved in the subpathway of pyrimidine metabolism that synthesizes UMP from uridine. Therefore, the suppression of *udk* might result in a higher uridine level in the intracellular extracts (Reaves, Young, Hosios, Xu, & Rabinowitz, 2013). The results also indicated that there was a significant difference between the EW treated and control cells in the transcription of glutamate decarboxylase gene, *gadA*, which encodes glutamate decarboxylase alpha. This enzyme converts glutamate to gamma-aminobutyrate (GABA), consuming one intracellular proton in the reaction. The *gad* system is critical to the survival of *E. coli* O157:H7 when cells are exposed to acidic conditions (Damiano et al., 2015; Foster, 2004). With regard to some genes (*oxyR*, *soxR*, *rpoH*, *gadA*, *sucA*), a similar observation was observed in non-pathogenic *E. coli*. Here, we observed differences among groups in the transcription levels of genes; however, these levels were not highly correlated with metabolites among groups, suggesting that other factors also contribute to the metabolic process.

4. Conclusion

The synergistic bactericidal effects of temperature and EW on antibacterial efficacy and ROS generation in *E. coli* O157:H7 EDL 933 and nonpathogenic *E. coli* were demonstrated. The results showed that heat

treatment causes a progressive increase of ROS in the presence of EW in *E. coli* cells. MS provides a sensitive and reproducible approach for metabolic profiling. The combined metabolomic and transcriptomic analysis of *E. coli* O157:H7 EDL 933 in response to EW and heat stresses caused synergistic conserved and specific cellular effects. The analysis of the results of combined treatment with EW and heat confirmed and extended existing mechanisms concerning gene expression and metabolites levels. Thus, the present results provide scientific evidence that a low concentration of EW combined with mild heat might be an effective control measure to minimize the risk of an *E. coli* O157:H7 outbreak.

Author contributions

Qin Liu designed this study, interpreted the results and drafted the manuscript. Lin Chen, Yun He and Xiao Feng did part of bacterial inactivation experiment. Anna K. C. Laserna conducted part of UPLC-QTOF-MS/MS experiment and interpreted the results. Dr. Hongshun Yang supervised the project and revised the manuscript.

Declaration of competing interest

The authors declare no conflict of interest associated with this study.

Acknowledgments

We acknowledge the financial support by Singapore Ministry of Education Academic Research Fund Tier 1 (R-143-000-A40-114),

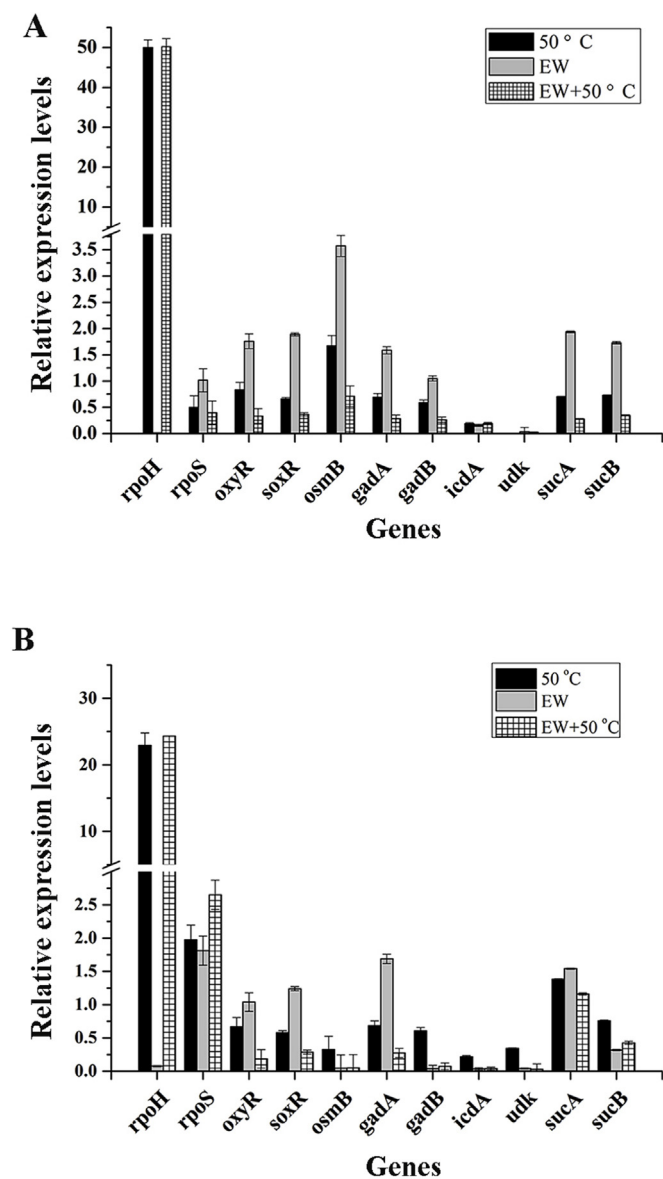


Fig. 7. Effect of electrolyzed water (EW) and heat treatment on gene expression of *Escherichia coli* O157:H7 EDL 933 (A) and nonpathogenic *E. coli* (B). Relative gene expression represents the change in transcription compared to the bacteria without treatment (control, value of 1.0). The expression of each gene was normalized to the expression of 16S rRNA in each sample. Data are expressed as the means \pm SD for RNA extracted in three replicates.

project 31371851 supported by NSFC, Natural Science Foundation of Jiangsu Province (BK20181184) and an industry project supported by Guangzhou Kaijie Power Supply Industry Co., Ltd (R-143-000-576-597).

Appendix A. Supplementary data

Supplementary data to this article can be found online at <https://doi.org/10.1016/j.foodcont.2019.107026>.

References

Adhikari, A., Yemmireddy, V. K., Costello, M. J., Gray, P. M., Salvadalena, R., Rasco, B., et al. (2018). Effect of storage time and temperature on the viability of *E. coli* O157:H7, *Salmonella* spp., *Listeria innocua*, *Staphylococcus aureus*, and *Clostridium sporogenes* vegetative cells and spores in vacuum-packed canned pasteurized milk cheese. *International Journal of Food Microbiology*, 286, 148–154.

Bolin, C., & Cardozo-Pelaez, F. (2007). Assessing biomarkers of oxidative stress: Analysis of guanosine and oxidized guanosine nucleotide triphosphates by high performance liquid chromatography with electrochemical detection. *Journal of Chromatography B*, 856, 121–130.

Chen, L., Zhao, X., Wu, J. E., He, Y., & Yang, H. (2020). Metabolic analysis of salicylic acid-induced chilling tolerance of banana using NMR. *Food Research International*, 108796.

Chen, X., & Hung, Y. C. (2017). Effects of organic load, sanitizer pH and initial chlorine concentration of chlorine-based sanitizers on chlorine demand of fresh produce wash waters. *Food Control*, 77, 96–101.

Chhetri, V. S., Fontenot, K., Strahan, R., Yemmireddy, V. K., Cason, C., Kharel, K., et al. (2019). Attachment strength and on-farm die-off rate of *Escherichia coli* on watermelon surfaces. *PLoS One*, 14(1), e0210115.

Chhetri, V. S., Janes, M. E., King, J. M., Doerrler, W., & Adhikari, A. (2019). Effect of residual chlorine and organic acids on survival and attachment of *Escherichia coli* O157: H7 and *Listeria monocytogenes* on spinach leaves during storage. *Lebensmittel-Wissenschaft und -Technologie- Food Science and Technology*, 105, 298–305.

Chung, H. J., Bang, W., & Drake, M. A. (2006). Stress response of *Escherichia coli*. *Comprehensive Reviews in Food Science and Food Safety*, 5, 52–64.

Cui, H., Bai, M., Yuan, L., Surendhiran, D., & Lin, L. (2018). Sequential effect of phages and cold nitrogen plasma against *Escherichia coli* O157:H7 biofilms on different vegetables. *International Journal of Food Microbiology*, 268, 1–9.

Damiano, M. A., Bastianelli, D., Dahouk, S. A., Köhler, S., Cloeckaert, A., Biase, D. D., et al. (2015). Glutamate decarboxylase-dependent acid resistance in *Brucella* spp.: Distribution and contribution to fitness under extremely acidic conditions. *Applied and Environmental Microbiology*, 81, 578–586.

Endersen, L., Coffey, A., Ross, R. P., McAuliffe, O., Hill, C., & O'Mahony, J. (2015). Characterisation of the antibacterial properties of a bacterial derived peptidoglycan hydrolase (LysCs4), active against *C. sakazakii* and other Gram-negative food-related pathogens. *International Journal of Food Microbiology*, 215, 79–85.

Ezraty, B., Gennaris, A., Barras, F., & Collet, J. F. (2017). Oxidative stress, protein damage and repair in bacteria. *Nature Reviews Microbiology*, 15, 385.

Farrés, M., Piña, B., & Tauler, R. (2016). LC-MS based metabolomics and chemometrics study of the toxic effects of copper on *Saccharomyces cerevisiae*. *Metall*, 8(8), 790–798.

Fei, F., Bowdish, D. M. E., & McCarty, B. E. (2014). Comprehensive and simultaneous coverage of lipid and polar metabolites for endogenous cellular metabolomics using HILIC-TOF-MS. *Analytical and Bioanalytical Chemistry*, 406, 3723–3733.

Fisher, K. D., Bratcher, C. L., Jin, T. Z., Bilgili, S. F., Owsley, W. F., & Wang, L. (2016). Evaluation of a novel antimicrobial solution and its potential for control *Escherichia coli* O157: H7, non-O157: H7 shiga toxin-producing *E. coli*, *Salmonella* spp., and *Listeria monocytogenes* on beef. *Food Control*, 64, 196–201.

Foster, J. W. (2004). *Escherichia coli* acid resistance: Tales of an amateur acidophile. *Nature Reviews Microbiology*, 2, 898–907.

Gil, M. I., Gómez-López, V. M., Hung, Y. C., & Allende, A. (2015). Potential of electrolyzed water as an alternative disinfectant agent in the fresh-cut industry. *Food and Bioprocess Technology*, 8, 1336–1348.

Han, D., Hung, Y. C., Bratcher, C. L., Monu, E. A., Wang, Y., & Wang, L. (2018). Formation of sublethally-injured *Yersinia enterocolitica*, *Escherichia coli* O157:H7, and *Salmonella enteritidis* cells after neutral electrolyzed oxidizing water treatments. *Applied and Environmental Microbiology*, 84(17), e01066-18.

Holmes, E., Want, E. J., Wilson, I. D., Plumb, R. S., Shockey, J., Nicholson, J. K., et al. (2010). Global metabolic profiling procedures for urine using UPLC-MS. *Nature Protocols*, 5, 1005–1018.

Horinouchi, N., Ogawa, J., Kawano, T., Sakai, T., Saito, K., Matsumoto, S., et al. (2006). Biochemical retrosynthesis of 2'-deoxyribonucleosides from glucose, acetaldehyde, and a nucleobase. *Applied Microbiology and Biotechnology*, 71, 615.

Joshi, I., Salvi, D., Schaffner, D. W., & Karwe, M. V. (2018). Characterization of microbial inactivation using plasma-activated water and plasma-activated acidified buffer. *Journal of Food Protection*, 81, 1472–1480.

Kaczmarczyk, A., Hochstrasser, R., Vorholt, J. A., & Francez-Charlot, A. (2015). Two-tiered histidine kinase pathway involved in heat shock and salt sensing in the general stress response of *Spingomonas melonis* Fr1. *Journal of Bacteriology*, 197(8), 1466–1477.

Levine, R. L., Moskovitz, J., & Stadtman, E. R. (2000). Oxidation of methionine in proteins: Roles in antioxidant defense and cellular regulation. *IUBMB Life*, 50, 301–307.

Liu, Q., Jin, X., Feng, X., Yang, H., & Fu, C. (2019). Inactivation kinetics of *Escherichia coli* O157: H7 and *Salmonella typhimurium* on organic carrot (*Daucus carota* L.) treated with low concentration electrolyzed water combined with short-time heat treatment. *Food Control*, 106, 106702.

Liu, Q., Tan, C. S. C., Yang, H., & Wang, S. (2017). Treatment with low-concentration acidic electrolyzed water combined with mild heat to sanitise fresh organic broccoli (*Brassica oleracea*). *LWT-Food Science and Technology*, 79, 594–600.

Liu, Q., Wu, J., Lim, Z. Y., Aggarwal, A., Yang, H., & Wang, S. (2017). Evaluation of the metabolic response of *Escherichia coli* to electrolyzed water by ^1H NMR spectroscopy. *Lebensmittel-Wissenschaft und -Technologie- Food Science and Technology*, 79, 428–436.

Liu, Q., Wu, J., Lim, Z. Y., Lai, S., Lee, N., & Yang, H. (2018). Metabolite profiling of *Listeria innocua* for unravelling the inactivation mechanism of electrolyzed water by nuclear magnetic resonance spectroscopy. *International Journal of Food Microbiology*, 271, 24–32.

Livak, K. J., & Schmittgen, T. D. (2001). Analysis of relative gene expression data using real-time quantitative PCR and the $2^{-\Delta\Delta\text{CT}}$ method. *Methods*, 25, 402–408.

Lu, W., Kimball, E., & Rabinowitz, J. D. (2006). A high-performance liquid chromatography-tandem mass spectrometry method for quantitation of nitrogen-containing intracellular metabolites. *Journal of the American Society for Mass Spectrometry*, 17(1), 37–50.

Mansilla, M. C., & de Mendoza, D. (2017). Regulation of membrane lipid homeostasis in

- bacteria upon temperature change. *Biogenesis of Fatty Acids, Lipids and Membranes*, 1–3.
- Marcén, M., Ruiz, V., Serrano, M. J., Condón, S., & Mañas, P. (2017). Oxidative stress in *E. coli* cells upon exposure to heat treatments. *International Journal of Food Microbiology*, *241*, 198–205.
- Mei, G. Y., Tang, J., Carey, C., Bach, S., & Kostrzynska, M. (2015). The effect of oxidative stress on gene expression of Shiga toxin-producing *Escherichia coli* (STEC) O157:H7 and non-O157 serotypes. *International Journal of Food Microbiology*, *215*, 7–15.
- Milligan, J., Aguilera, J., & Ward, J. (2001). Redox equilibrium between guanyl radicals and thiocyanate influences base damage yields in gamma irradiated plasmid DNA. Estimation of the reduction potential of guanyl radicals in plasmid DNA in aqueous solution at physiological ionic strength. *International Journal of Radiation Biology*, *77*, 1195–1205.
- Montville, R., & Schaffner, D. W. (2004). Analysis of published sprout seed sanitization studies shows treatments are highly variable. *Journal of Food Protection*, *67*, 758–765.
- Ngnitcho, P. F. K., Tango, C. N., Khan, I., Daliri, E. B. M., Chellian, R., & Oh, D. H. (2018). The applicability of Weibull model for the kinetics inactivation of *Listeria monocytogenes* and *Escherichia coli* O157:H7 on soybean sprouts submitted to chemical sanitizers in combination with ultrasound at mild temperatures. *Lebensmittel-Wissenschaft und -Technologie- Food Science and Technology*, *91*, 573–579.
- Reaves, M. L., Young, B. D., Hosios, A. M., Xu, Y. F., & Rabinowitz, J. D. (2013). Pyrimidine homeostasis is accomplished by directed overflow metabolism. *Nature*, *500*, 237–241.
- Sévin, D. C., & Sauer, U. (2014). Ubiquinone accumulation improves osmotic-stress tolerance in *Escherichia coli*. *Nature Chemical Biology*, *10*, 266–272.
- Sheridan, G. E. C., Masters, C. I., Shallcross, J. A., & Mackey, B. M. (1998). Detection of mRNA by reverse transcription-PCR as an indicator of viability in *Escherichia coli* cells. *Applied and Environmental Microbiology*, *64*(4), 1313–1318.
- Stadtman, E. R., Moskovitz, J., Berlett, B. S., & Levine, R. L. (2002). Cyclic oxidation and reduction of protein methionine residues is an important antioxidant mechanism, p3–9. In V. Vallyathan, X. Shi, & V. Castranova (Eds.). *Oxygen/nitrogen radicals: Cell injury and disease. Developments in molecular and cellular biochemistry*. Boston, MA: Springer.
- Stan, S. D., Woods, J. S., & Daeschel, M. A. (2005). Investigation of the presence of OH radicals in electrolyzed NaCl solution by electron spin resonance spectroscopy. *Journal of Agricultural and Food Chemistry*, *53*, 4901–4905.
- Stincone, A., Prigione, A., Cramer, T., Wamelink, M. M. C., Campbell, K., Cheung, E., et al. (2015). The return of metabolism: Biochemistry and physiology of the pentose phosphate pathway. *Biological Reviews of the Cambridge Philosophical Society*, *90*, 927–963.
- Tam, E. W. T., Chen, J. H. K., Lau, E. C. L., Ngan, A. H. Y., Fung, K. S. C., Lee, K. C., et al. (2014). Misidentification of *Aspergillus nomius* and *Aspergillus tamarii* as *Aspergillus flavus*: Characterization by internal transcribed spacer, β -tubulin, and calmodulin gene sequencing, metabolic fingerprinting, and matrix-assisted laser desorption ionization-time of flight mass spectrometry. *Journal of Clinical Microbiology*, *52*, 1153–1160.
- Tango, C. N., Mansur, A. R., Kim, G. H., & Oh, D. H. (2014). Synergetic effect of combined fumaric acid and slightly acidic electrolysed water on the inactivation of food-borne pathogens and extending the shelf life of fresh beef. *Journal of Applied Microbiology*, *117*, 1709–1720.
- Wang, S., Deng, K., Zaremba, S., Deng, X., Lin, C., Wang, Q., et al. (2009). Transcriptomic response of *Escherichia coli* O157:H7 to oxidative stress. *Applied and Environmental Microbiology*, *75*(19), 6110–6123.
- Yang, Y., Khoo, W. J., Zheng, Q., Chung, H. J., & Yuk, H. G. (2014). Growth temperature alters *Salmonella* Enteritidis heat/acid resistance, membrane lipid composition and stress/virulence related gene expression. *International Journal of Food Microbiology*, *172*, 102–109.
- Zampieri, M., Sekar, K., Zamboni, N., & Sauer, U. (2017). Frontiers of high-throughput metabolomics. *Current Opinion in Chemical Biology*, *36*, 15–23.
- Zhao, L., Zhao, X., Wu, J. E., Lou, X., & Yang, H. (2019). Comparison of metabolic response between the planktonic and air-dried *Escherichia coli* to electrolysed water combined with ultrasound by ^1H NMR spectroscopy. *Food Research International*, *125*, 108607.
- Zook, C. D., Busta, F. F., & Brady, L. J. (2001). Sublethal sanitizer stress and adaptive response of *Escherichia coli* O157:H7. *Journal of Food Protection*, *64*, 767–769.